

Thermal bilateral coupling in teleoperators

A. Drif*, J. Citérin* and A. Kheddar*[§]

*Laboratoire Systèmes Complexes
Université d'Evry - CNRS, France

Email: adrif,citerin,kheddar@iup.univ-evry.fr

[§]AIST/CNRS Joint Robotics Laboratory (JRL)

ISRI Central 2, Tsukuba, Japan

Email: kheddar@ieee.org

Abstract—This paper presents a new method and formalism to achieve thermal feedback for teleoperation and telepresence applications. The basic idea is to realize an approach similar to force reflecting telerobotics. That is to say, bilateral coupling between thermal temperature and thermal flux variables. Thermal properties and exchange during contact are modeled with their relating equations. Similarly to force feedback coupling, four potential controllers are possible; we implemented all of them using stable and linear control schemes. Experimental results show that some coupling are superior in terms of thermal transparency and stability. We used two Peltier heat pumps as thermal sources; the one serving as a thermal display while the other one is to play the role of a “robotic finger”.

I. INTRODUCTION AND PREVIOUS WORK

Thermal feedback for teleoperators has not been extensively investigated in comparison with force feedback. Russel, [1] [2] conceived thermal sensors based on heat exchange occurring when contact is made between two objects of different materials. The purpose was remote materials identification. Each sensor comprises a heating source to warm the unknown material and an array of temperature transducers to measure contact point's temperature over the sensor. These measures are compared with a library of temperature profile constructed from known materials.

In [3], an exoskeleton teleoperation system is developed; this system integrates temperature sensors in a teleoperator arm, a tactile feedback glove is used to control this arm. This master glove feeds the temperature on the back surface of the user's index finger. Another interface has been developed at the Hokkaido university; this interface used heat-element based on Peltier effect to warm and cold the operator's finger. Authors study the capacity of an operator to identify various material, the discrimination factor was found to depend strongly on the temporal evolution of the temperature difference. In [4], a Peltier pump is integrated as part of the force feedback on the PHANTOM. The device achieves heating and cooling rates of $+11^{\circ}\text{C}/\text{sec}$ and $-4.5^{\circ}\text{C}/\text{sec}$ respectively.

Recent approaches used the physiological composition of the human finger (bone, blood and skin) and thermo-electricity laws to model and explain the heat exchange that occurs in each part of the finger when touching an object. In [5], an artificial robotic finger is developed for research in car industry. The device is used for measuring temperature by mean of sensors placed in an elastomer that have thermal

properties near of that of the human finger. A similar analogy is presented in [6] for presenting a thermal feedback model in virtual reality, the model of heat exchange between the finger skin and a material are established by electrical analogy, this model takes in consideration conduction and convection of air around the finger and around the touched material, see also [7] for modeling the thermal contact phenomena for tactile feedback in virtual environments applications, and [8] for temperature rendering based on contact temperature prediction and human finger effusivity.

Most of proposed thermal feedback schemes used temperature coupling controlling a heat source to reproduce a desired temperature. Nevertheless, the most pertinent parameter in thermal perception is in the temperature ‘diffusion’ rate. Moreover, their simplified models applies only at the steady state phase i.e when the thermal equilibrium is reached.

Thermal exchange dynamics is perceptually the most pertinent issue. It occurs however at the transition phases i.e. before reaching thermal equilibrium. The present work gives a new approach and formalism in the implementation of the thermal rendering for teleoperators using the bilateral coupling early established in force reflecting systems. The developed system is used for thermal rendering and thermal identification of remote touched objects. To catch the transition phase dynamics, a dedicated electronic board has been conceived in order to drive the Peltier pumps at high sampling rates.

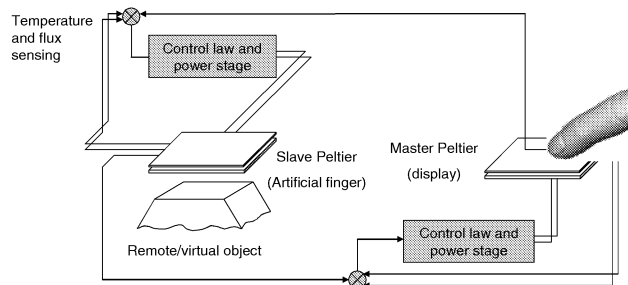


Fig. 1. The thermal teleoperator.

II. MODELING OF THE THERMAL MASTER/SLAVE SYSTEM

The perception of the heat flux transferred at the contact space/interface is mainly affected by the temperature rate

change and the heat transfer speed. The proposed thermal teleoperator uses two heat-controlled elements. Each of them is composed of a Peltier pump, as a heat source, temperature sensors, heat flux sensors (this has never been used before) and finally fast driving and sampling dedicated electronics.

The thermal teleoperator is composed of a master and a slave parts, Fig 1. The master uses one Peltier pump as a thermal display stimulating the operator finger. This Peltier is driven according to the temperature and the heat flux observed in the slave part. The slave part uses the second Peltier pump to heat the touched object; it is driven according to the temperature and the heat flux observed in the master part. In this way, we aim at reproducing in a most transparent way thermal sensations experienced in both sides with a minimum modeling of the thermal effects.

A. Basic thermal contact equations

Modeling thermal exchange in terms of heat flux, allows to determine the temperature evolution in time and space dimensions. In normal situations, heat flows by conduction from warmer material into a cooler material until their temperature equalizes (Fig 2). The instantaneous change in temperature depends on the temperature difference between the two materials and on their thermal conductivity. The heat energy flows also by convection and radiation. In our case, when the contact is established, the conduction phenomenon is dominant.

The heat equation is given for one dimension, according to the heat transfer direction, since 2D heat exchange model can be approximated to a mono-directional-conductive heat exchange [5]. If two objects of different materials are made in contact, the heat quantity transmitted by conduction is formulated, at the limit of the contact area, by:

$$\varphi = -\lambda \nabla T = -\lambda S \frac{\partial T}{\partial x} \quad (1)$$

where φ is the heat flux across the contact area [$\text{W} = \text{J}/\text{sec}$], λ is the material conductivity [$\text{Wm}^{-1}\text{K}^{-1}$], x is the heat transfer direction [m], and S is the section area [m^2].

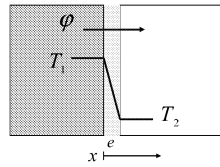


Fig. 2. The heat flux transfer between two blocks material.

The temperature evolution for each material is:

$$\frac{\partial T_i(x, t)}{\partial t} = a \frac{\partial^2 T_i(x, t)}{\partial x^2} \quad (2)$$

where the subscribe i states for material 1 and 2 respectively, and a is the thermal diffusivity. The temperature increase of the coldest material and temperature diminution of the warmer

one corresponds to the quantity of the heat stocked or released by each material respectively, this quantity of heat is:

$$\varphi = \rho V c_v \frac{\partial T}{\partial t} \quad (3)$$

where φ is the quantity of heat flux stocked [W], ρ is the material density [kg m^{-3}], V is the volume [m^{-3}], c_v is the specific heat at constant volume [$\text{J kg}^{-1}\text{K}^{-1}$]. In the contact area limit, when the transfer is permanent, the heat flux is equal along the x axis, that is $\varphi_x = \varphi_{x+dx}$ and the temperature equation becomes [9]:

$$a \frac{\partial^2 T(x, t)}{\partial x^2} = 0 \quad (4)$$

The general solution of that equation is $T(x) = c_1 x + c_2$, with the boundary conditions $T_{x=0} = T_1$ and $T_{x=e} = T_2$ where e is the contact area thickness [m], we have:

$$T = T_1 - \frac{x}{e}(T_1 - T_2) \quad (5)$$

The temperature profile is linear and the heat flux is:

$$\varphi = \frac{\lambda S(T_1 - T_2)}{e} = \frac{(T_1 - T_2)}{e/\lambda S} \quad (6)$$

By analogy with the Ohm's law in electricity, the temperature difference ($T_1 - T_2$) between two given points in each side, creates a temperature flux φ between these two points; this is equivalent to an electrical potential difference applied to the two ends of a resistance. Thus, $R_{th} = \frac{e}{\lambda S}$ is called the thermal resistance, and is expressed in [$^{\circ}\text{K}/\text{J sec}^{-1}$].

Under the influence of the temperature difference ($T_1 - T_2$), the heat flux increases the temperature of the cold points in the contact area trying to reach equilibrium. This occurs after a period of time which is equivalent to the loading time of a capacitor. This is expressed by:

$$\frac{\partial T}{\partial t} = \frac{1}{c} \varphi \quad (7)$$

where c is the thermal capacity expressed in [$\text{W sec } ^{\circ}\text{C}$], and can be calculated for a sample material by $c = mc_v$; c_v is the specific heat at a constant volume and m is the material mass.

B. Master part

It is composed by the operator finger, the thermal display (Peltier pump) and the temperature/heat flux sensors, Fig 3.

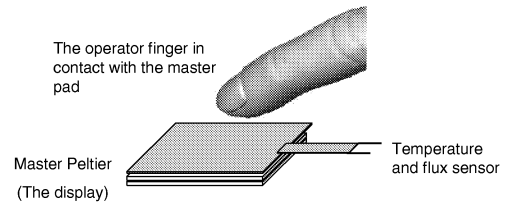


Fig. 3. The master with temperature and heat flux sensor placement.

The heat flux φ_m between the finger and the display is:

$$\varphi_m = \frac{1}{R_m} (T_h - T_d) \quad (8)$$

and the temperatures evolutions are:

$$\frac{\partial T_h}{\partial t} = \frac{1}{c_h} \varphi_m \quad (9)$$

$$\frac{\partial T_d}{\partial t} = \frac{1}{c_d} \varphi_m \quad (10)$$

subscribe h designates human and d the thermal display.

C. The slave part

It is composed by a Peltier pump having the role of a robotic finger and the temperatures/heat flux sensors, Fig 4.

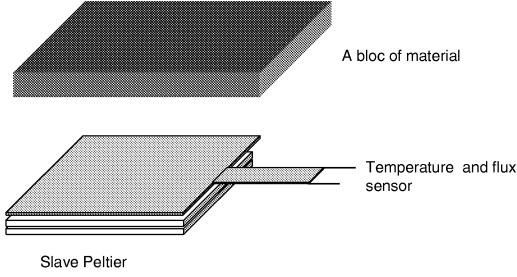


Fig. 4. The slave part with temperature and heat flux sensors.

The heat flux between the artificial finger and the touched object is:

$$\varphi_s = \frac{1}{R_s} (T_s - T_o) \quad (11)$$

and the temperatures evolutions are similarly:

$$\frac{\partial T_s}{\partial t} = \frac{1}{c_s} \varphi_s \quad (12)$$

$$\frac{\partial T_o}{\partial t} = \frac{1}{c_o} \varphi_s \quad (13)$$

subscribe s designates the robotic finger and o the object.

The resolution of the above equations shows that the initial temperature values for each part affect the evolution of the temperature and the heat flux. Thus, the final value reached in equilibrium in the contact area between two known materials can be estimated using the temperature contact equation, that is $T_c = \frac{E_1 T_1 + E_2 T_2}{E_1 + E_2}$, where T and E are the material temperature and the material thermal effusivity respectively.

The two parts of the teleoperator are simulated under Matlab/Simulink™ environment without any control law. The values of the different constants are set before the simulation starts and are taken from the material thermal properties table [10] and from the human biophysics data. The Fig 5 shows the simulated plotted curves corresponding to the following initial conditions $T_h = 37^\circ\text{C}$, $T_d = 25^\circ\text{C}$, $T_s = 17^\circ\text{C}$ and $T_o = 15^\circ\text{C}$.

It is clear that to reach a good transparency, the display temperature must copy the object temperature evolution, and the artificial finger temperature evolution must copy the operator finger temperature. For this aim, a control law is used in the master display and the slave Peltier. Both, must have the same final temperature values and the same thermal dynamics.

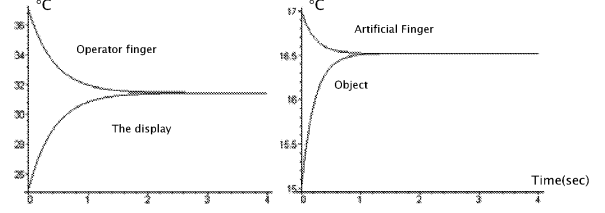


Fig. 5. Temperature evolution in the master and the slave.

This means that the heat flux in the master part must equal the heat flux in the slave part. The results of the simulations with controlling the two temperatures are shown on Fig 6.

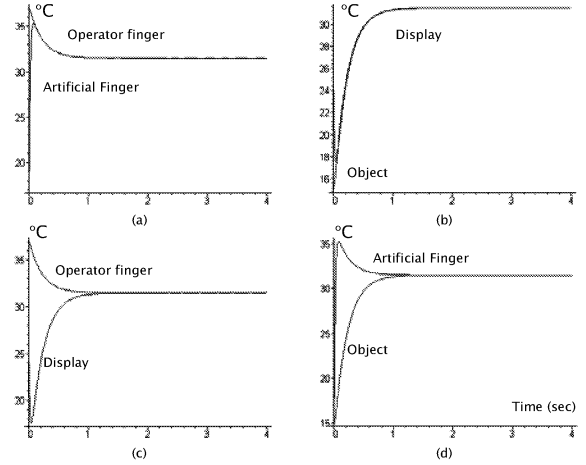


Fig. 6. The master and slave controlled temperature evolution. (a) the artificial finger controlled with the operator finger temperature. (b) display temperature controlled with the object temperature. (c) temperature evolution in the master part. (d) temperature evolution in the slave part.

D. Modeling the Peltier pump

Although commercially available, the main problem of Peltier pumps is to have a simple and accurate dynamic equations that directly link the voltage supply feeding the Peltier pump and the temperature of each Peltier pump' sides. Theses equations are hard to obtain, and an exhaustive analysis of the electro-thermal Peltier effect is difficult because of the nonlinear behavior of the Peltier effect that acts as a floating load for the voltage supply and the several nonlinear phenomena that occur within it.

A standard Peltier pump behavior can be described by two basic equations determining the heat transfer rate and the maximum difference temperature between the two sides, these equations are:

$$\varphi = \alpha_p I (T_{hot} - T_{cold}) - KI^2 \quad (14)$$

$$(T_{hot} - T_{cold})_{max} = \frac{\alpha^2 T_{hot}^2}{2KR} \quad (15)$$

where $T_{hot,cold}$ [$^{\circ}\text{K}$] are the temperature of the hot and the cold side respectively, I [A] is the electrical current passed through the Peltier thermocouple, α [$\mu\text{V}/^{\circ}\text{K}$] is the Seebeck coefficient, R [Ω] and K [$\text{W}/^{\circ}\text{K}$] are respectively the total electrical resistance and the total thermal conductance for both p - and n - element of the Peltier pump, defined as:

$$R = N \left(\frac{\rho_n L_n}{A_n} + \frac{\rho_p L_p}{A_p} \right) \quad (16)$$

$$K = N \left(\frac{\lambda_n A_n}{L_n} + \frac{\lambda_p A_p}{L_p} \right) \quad (17)$$

where ρ [$\mu\Omega\text{m}$] is the Peltier material resistivity, A [m^2] and L [m] are respectively the cross section and the length of the thermocouple element, N is the total number of the p - and n - type junction, and λ [$\text{W m}^{-1}\text{K}^{-1}$] is the thermal conductivity of the Peltier junction material.

We assume that the Peltier pump properties are stationary. The cold side is closed-up with a dissipater having high thermal conductivity to assume T_{cold} constant and close to the room temperature.

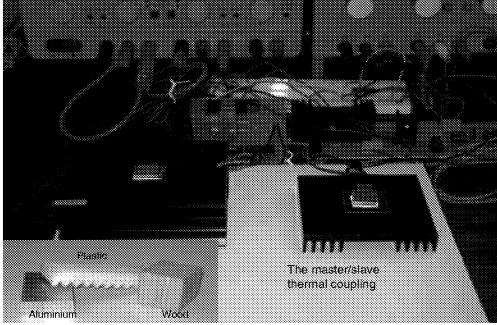


Fig. 7. The thermal teleoperator setup.

E. Experimental setup design and parameters seatings

The Fig 7 shows the experimental setup. The master part consist of a contact pad using a Peltier pump $15\text{mm} \times 15\text{mm} \times 3.2\text{mm}$ from MELCORTM with the characteristic parameters summarized in the table I. A CAPTECTM heat flux sensor with an integrated thermocouple type T $15\text{mm} \times 15\text{mm} \times 420\mu\text{m}$ is assembled at the contact interface.

Material properties	Values
Seebeck Coefficient α [$\text{V}/^{\circ}\text{K}$]	$2.02 \cdot 10^{-4}$
Resistivity ρ [Ωcm]	$1.01 \cdot 10^{-3}$
Conductivity λ [$\text{W}/\text{cm}^{\circ}\text{K}$]	$1.51 \cdot 10^{-2}$
Junction Number N	31
Element Type Section A [mm^2]	1
Element Type Length L [mm]	1.6

TABLE I
THE PELTIER DEVICE PROPERTIES.

A silicone grease is used to decrease the thermal resistance between the Peltier surface and (i) the heat flux sensor, and (ii) the dissipater. This reduces thermal loss.

The Fig 8 show the control signal flow in both sides. The controller block is driving from an IO board, which monitors the I/O signals, detects the contact instant in the slave part and switches the control mode.

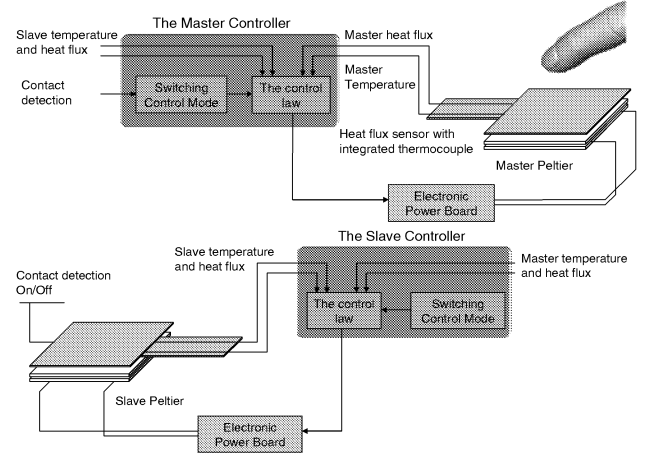


Fig. 8. Diagram of the master and slave controllers.

The instant contact in the slave Peltier is determined thanks to an On/Off pressure sensor placed under Peltier surface.

III. BILATERAL CONTROLLER DESIGN

This section addresses the bilateral thermal feedback and its implementation in a four-channel teleoperator control architecture. As in teleoperation system, we follow the analogy used in mechanical and electrical systems relating the temperature to the effort variable (force or voltage) and the heat flux to the flow variable (position or current). The novel idea is to use similar bilateral coupling schemes under the objectives of thermal transparency while maintaining stability.

The dynamic of the operator finger is not modeled here because it is complicated to illustrate, this dynamic is variable and is especially subject-dependent, time-dependent and contact-dependent. In the work presented in [11], the human finger temperature is estimated when the contact is made with a material with known thermal properties by resolving a heavy PDE system.

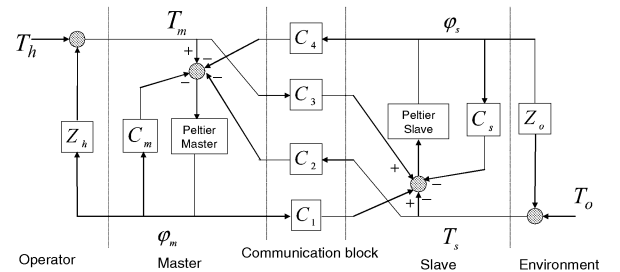


Fig. 9. Block diagram of a four-channel thermal teleoperator.

The Fig 9 shows a general thermal teleoperation system adapted from [12]. The connection between the different

blocks is adopted in a conventional manner where $C_{m,s}$ denote the master and slave local controllers, $Z_{h,o}$ denote the operator and the object thermal impedance and $\varphi_{m,s}$ denote the master and slave heat flux.

The four-coupling schemes are implemented with objects made by materials with different thermal conductivity and diffusivity (aluminum, wood and plastic).

A. Thermal flux/flux coupling

In the flux-flux coupling scheme (the controllers $C_2 = C_3 = 0$ in the Fig 9), the master is regulated to reproduce the slave heat flux and conversely. Initially, the operator is in contact with the display. Since the finger is continuously thermo-regulated by blood circulation, the thermal sensation experienced by the finger is altered and the operator feels the thermal change even if there were not remote object touched. To tackle this, the master initial temperature is first regulated in the temperature range 29–35°C, this range is known as *the thermal neutral* or *the physiological zero* [13], since no thermal sensation is experienced when the finger temperature is changing slowly within this range (complete thermal adaptation). When the remote contact is made, the induced signal starts the regulation according to the heat flux evolution. The control law applied are defined as:

$$\tau_m = C_m (\varphi_s - \varphi_m) \quad (18)$$

$$\tau_s = C_s (\varphi_m - \varphi_s) \quad (19)$$

where $C_{m,s} = k_p + k_d s + k_i/s$, k_p , k_d , k_i are the controller gain and s states for the Laplace variable, the remaining $C_{1,4}$ are chosen as unity gains. The experimental curves are plotted on Fig 10.

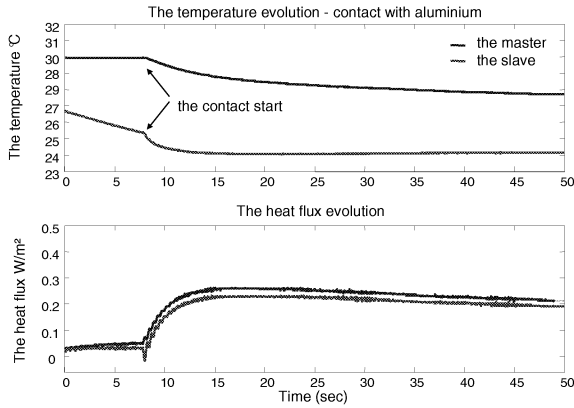


Fig. 10. The thermal heat-flux/flux coupling mode.

B. Thermal flux/temperature coupling

This is the flow/effort control scheme; known as admittance rendering [14]. In this coupling scheme, the temperature feed-forwards from the slave to the master and the flux feed-forwards from the master to the slave ($C_1 = C_2 = 0$). We follow the same steps as the previous coupling scheme, when

the slave is not in contact, the master is controlled in the thermal neutral range. If a contact is detected by the pressure sensor, the heat flux measured by the slave heat flux sensor is fed back to the master controller as reference, and the master temperature generated by the master heat flux variation is send to the slave controller as a reference. The control laws are defined as:

$$\tau_m = C_m (\varphi_s - \varphi_m) \quad (20)$$

$$\tau_s = C_s (T_m - T_s) \quad (21)$$

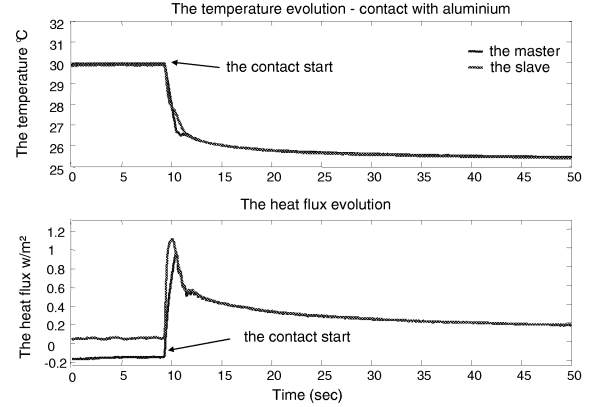


Fig. 11. The thermal heat-flux/temperature coupling mode.

C. Thermal temperature/temperature coupling

In the temperature/temperature coupling scheme noted as the effort/effort control architecture ($C_1 = C_4 = 0$ in the Fig 9). In this structure, no consideration is given to heat flux. The control law applied are defined as:

$$\tau_m = C_m (T_s - T_m) \quad (22)$$

$$\tau_s = C_s (T_m - T_s) \quad (23)$$

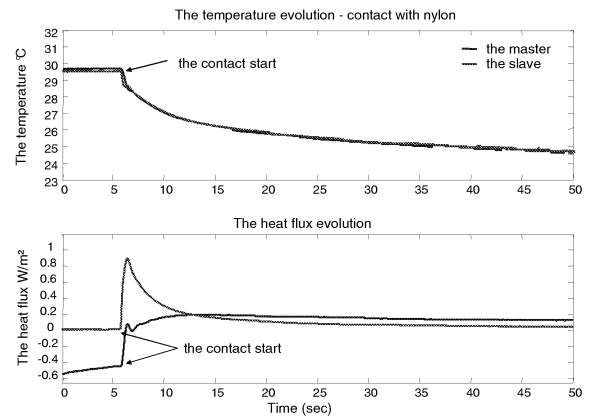


Fig. 12. The thermal temperature/temperature coupling mode.

The experimental curves revealed from the contact of the slave with nylon block is shown on the Fig 12.

D. Thermal temperature/flux coupling

In the temperature-flux coupling scheme, also known as *flow forward structure* [12], the slave contact temperature is fed back to the master and the heat flux of the master is send to the slave controller as a reference ($C_3 = C_4 = 0$). The controllers applied for the master and the slave are defined as:

$$\tau_m = C_m (T_o - T_m) \quad (24)$$

$$\tau_s = C_s (\varphi_m - \varphi_s) \quad (25)$$

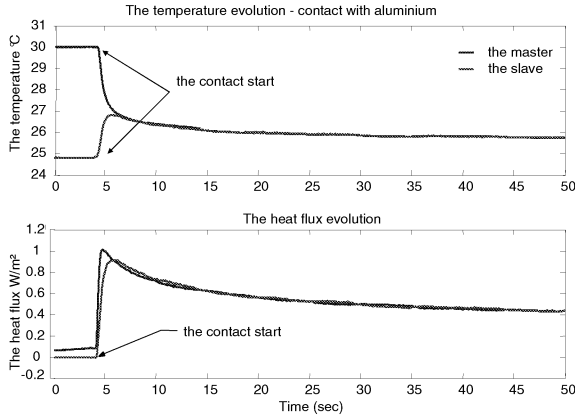


Fig. 13. The thermal temperature/heat-flux coupling mode

IV. DISCUSSION

In thermal flux/flux coupling scheme, as shown on Fig 10, while the heat flux generated by the real contact with the material object is the same that is reproduced in the master and felt by the operator, the temperatures curves can evolve differently. Thus several tests on different materials in different room temperature initial condition show that the operator can feel warm while the object touched by the slave is cold. This is mainly due to the relation between the temperature and the heat flux (see equation 1) and the initial temperature in which is the slave. Small heat flux variations produced by the contact may lead to different temperature evolutions depending on actual temperature initial values. The relevant experiments shows that flux/flux scheme exhibits poor transparency and performance and the stability strongly depends on the contact nature, an abrupt heat flux variation may lead to temperature divergence.

Temperature/temperature scheme presents good sensibility (see Fig 12). The thermal transient that occurs when the slave comes in contact with the material object, is detected and felt by the operator finger. One distinguishes between two different material only when their thermal conductivity are largely different (e.g. aluminum and nylon or aluminum and wood). The same performance is reached with the flux/temperature coupling scheme (see Fig 11), which seem to be more sensitive to temperature change especially when the contact is with a material having small thermal conductivity (e.g. wood).

The last coupling scheme (Fig 13) do not add performance and the operator is more influenced by the contact with the heat-flux sensor material (the copper).

V. CONCLUSION

This paper proposes to conceive thermal feedback on the basic of force reflecting teleoperators. The preliminary obtained results need a more thorough investigations, namely:

- the influence of the material surface features (surface texture and roughness) on the contact;
- quantitative transparency and stability analysis based on passivity and non linear control, more refined system modeling and parameters' identification;
- thermal impedance shaping;
- human material discrimination performance;
- increase hardware performance, design a new display;
- inclusive haptic interface integration.

This study precludes further investigations and interests in thermal teleoperator with bilateral coupling.

ACKNOWLEDGMENT

This work is sponsored by TOUCH-HapSys project. Contract No. IST-2001-38040, action line IST-2002-6.1.1 (FET-Presence) www.touch-hapsys.org.

REFERENCES

- [1] R. A. Russell, "Thermal sensor for object shape and material constitution," *Robotica*, 1988.
- [2] R. A. Russell and F. J. Paoloni, "Robot sensor for measuring thermal properties of gripped objects," *IEEE Transactions on Instrumentation and Measurements*, 1985.
- [3] D. Caldwell, U. Andersen, C. Bowler, and A. Wardle, "A high power/weight dexterous manipulator using sensory glove based motion control and tactile feedback," *Transaction of the Institute of Measurement and Control*, 1995.
- [4] M. Ottensmeyer and J. Salisbury, "Hot and cold running vr, adding thermal stimuli to haptics experience," *Proceedings of the Phantom Users Group*, 1997.
- [5] R. Deterre, A. Sandra, and C. Vergneault, "Le doigt thermique : une réponse innovante à la caractérisation sensorielle des produits," *SIA*, 2002.
- [6] M. Benali-Khoudja, M. Hafez, J. M. Alexandre, and A. Kheddar, "Thermal feedback for virtual reality," *International Symposium on Micromechatronics and Human Science*, 2003.
- [7] M. Bergamasco, A. A. Alessi, and M. Calcara, "Thermal feedback in virtual environments," *Presence*, vol. 6, Issue 6, pp. 617-629, 1997.
- [8] A. Yamamoto, B. Cros, H. Hashimoto, and T. Higuchi, "Control of thermal tactile display based on prediction of contact temperature," *International Conference on Robotics and Automation*, 2004 New Orleans LA.
- [9] J. H. Lienhard and J. H. Lienhard, Eds., *A Heat Transfer TextBook*. Phlogiston Press, Cambridge, Massachusetts, USA., 2004.
- [10] H. S. Carslaw and J. C. Jaeger, Eds., *Conduction of heat in solids*. Oxford, Clarendon Press, Oxford University Press, 1959.
- [11] D. Hodson, J. Barbenel, and G. Eason, "Modeling transient heat transfer through the skin and a contact material," *Phys. Med. Biol.*, 1089.
- [12] D. A. Lawrence, "Stability and transparency in bilateral teleoperation," *IEEE Transactions on Robotics and Automation*, 1993.
- [13] H. R. Nicholls, Ed., *Advanced Tactile Sensing For Robotics*. World Scientific Publishing Co. Pte. Ltd, 1992.
- [14] R. Adams and B. Hannaford, "Stable haptic interaction with virtual environments," *IEEE Transactions on Robotics and Automation*, 1999.